

## Nanorod solar cell with an ultrathin a-Si:H absorber layer

Yinghuan Kuang,<sup>a)</sup> Karine H. M. van der Werf, Z. Silvester Houweling, and Ruud E. I. Schropp

Faculty of Science, Debye Institute for Nanomaterials Science, Section Nanophotonics, Utrecht University, P.O. Box 80.000, 3508 TA Utrecht, The Netherlands

(Received 2 February 2011; accepted 24 February 2011; published online 16 March 2011)

We propose a nanostructured three-dimensional (nano-3D) solar cell design employing an ultrathin hydrogenated amorphous silicon (a-Si:H) n-i-p junction deposited on zinc oxide (ZnO) nanorod arrays. The ZnO nanorods were prepared by aqueous chemical growth at 80 °C. The photovoltaic performance of the nanorod/a-Si:H solar cell with an ultrathin absorber layer of only 25 nm is experimentally demonstrated. An efficiency of 3.6% and a short-circuit current density of 8.3 mA/cm<sup>2</sup> were obtained, significantly higher than values achieved for planar or even textured counterparts with three times thicker (~75 nm) a-Si:H absorber layers. © 2011 American Institute of Physics. [doi:10.1063/1.3567527]

To achieve a high energy conversion efficiency, a solar cell must be thick enough for sufficient light absorption, yet it must be thin enough for efficient carrier collection.<sup>1-3</sup> Recently, the applications of nanocoax,<sup>1</sup> nanocone,<sup>4,5</sup> nanodome,<sup>6</sup> nanopillar,<sup>7,8</sup> nanorod,<sup>2,3,9-13</sup> and nanowire<sup>14-24</sup> structures for solar cells have attracted great interest. Compared to the conventional planar thin film counterparts, the nanostructured devices demonstrate the benefits of enhancing charge collection and improving light absorption simultaneously, due to their unique geometry. In the axial direction the absorber ensures sufficient light absorption, whereas in the radial direction it guarantees efficient carrier extraction.<sup>2</sup>

Among the nanostructured photovoltaic devices, Si nanowire-based radial p-n junction solar cells have attracted most attention. Si nanowires can be prepared by various approaches, such as wet chemical etching,<sup>18</sup> reactive ion etching,<sup>4,23</sup> and vapor-liquid-solid methods.<sup>15,17,19,20</sup> However, all these methods either use a Si-wafer as starting material or employ a high synthesis temperature, consequently it is uncertain whether these approaches will ultimately reduce material usage and/or energy consumption. In contrast, our approach focuses on a simple fabrication process at low temperature with low material usage. Zinc oxide (ZnO) nanorod arrays were used as the backbones because they can be easily prepared on various cheap substrates such as glass or even flexible plastic by solution-deposition at a temperature below 100 °C.<sup>25-29</sup> Furthermore, for the solution-deposition of ZnO nanorods, there is no substrate size limitation and no need for expensive and sophisticated lithographic techniques. We employ hydrogenated amorphous silicon (a-Si:H) as the absorber material rather than CdSe/CdTe,<sup>3,7</sup> In<sub>2</sub>S<sub>3</sub>,<sup>9,10</sup> CuInS<sub>2</sub>,<sup>11,12</sup> InP, and GaP,<sup>24</sup> since silicon is a nontoxic thin film photovoltaic material that is abundantly available.

Figure 1(a) represents a schematic of the nanorod solar cell design in a cross-sectional view. The ZnO nanorods were synthesized at 80 °C during 3 h in a mixed aqueous solution with a concentration of 0.0005 mol/L (M) zinc acetate dihydrate and 0.0005 M hexamethylenetetramine. After sputter-deposition of a flat ZnO seed layer on glass, the substrate was immersed in the solution, holding ZnO film side down-

ward. From the x-ray diffraction result (not shown) it is found that high-quality hexagonal single-crystal ZnO nanorods were prepared. The diameter of the nanorods calculated from high-resolution scanning electron microscopy (HRSEM) image (not shown) varies between 40 and 180 nm, with an average value of about 112 nm. The average length is approximately 400 nm and the site-density amounts to about  $7 \times 10^8/\text{cm}^2$ . A silver layer of a thickness of about 20 nm was sputtered over the nanorods, followed by a ZnO:Al transparent conductive oxide (TCO) layer of a thickness of about 38 nm. Then, the deposition of an a-Si:H n-i-p layer stack was carried out in a multichamber deposition system which is described elsewhere.<sup>30</sup> To provide conformal coverage, the intrinsic (i-) layer was deposited by hot-wire chemical vapor deposition (CVD) (Ref. 31) using SiH<sub>4</sub>:H<sub>2</sub> (30:60) as source gasses, whereas plasma-enhanced CVD was employed for the deposition of the p- and n-layers. B(CH<sub>3</sub>)<sub>3</sub> and PH<sub>3</sub> were utilized for p- and n-doping, respectively. The arrays were sputter-coated with 4 mm × 4 mm squares of transparent conducting indium tin oxide (ITO) layer of a thickness of 35 nm after the deposition of the a-Si:H n-i-p layers. Gold top-grid contacts were evaporated onto the square ITO pads defining the area of the cells, leaving an active cell area of 0.13 cm<sup>2</sup> for each cell. Figures 1(b) and 1(c) show HRSEM top-view (tilted 45°) and sectional-view images of the completed nanorod solar cells, respectively. The average thicknesses of the applied layers were determined by measuring the growth in diameter of the coated nanorods in HRSEM images after each individual layer deposition; Table I shows the results. The HRSEM imaging was performed with a Philips XL30SFEG microscope.

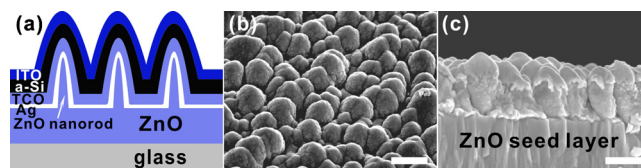


FIG. 1. (Color online) ZnO-nanorod/a-Si:H solar cells. (a) Cross-sectional schematic (not to scale). (b) HRSEM top-view image (tilted 45°) and (c) cross-sectional view image of a completed nanorod cell. All scale bars are 500 nm.

<sup>a)</sup>Electronic mail: y.kuang@uu.nl.

TABLE I. Thicknesses of the applied layers in nanometer in the three kinds of fabricated solar cells.

No.	Ag	TCO	i-layer	ITO
F75	100	100	75	80
T75	100	100	75	80
NR25	20	38	25	35

Figure 2(a) shows the current density-voltage ( $J$ - $V$ ) characteristics of the nanorod solar cells measured with a solar simulator under one sun illumination (AM1.5G, 100 mW/cm<sup>2</sup>). The data show, that with an ultrathin i-layer of a thickness of only about 25 nm, the nanorod solar cell (NR25) has an energy conversion efficiency ( $\eta$ ) of 3.6%, which is significantly higher than the 3.0% and 2.6% achieved for the textured and the planar counterparts that even have three times thicker i-layers of 75 nm. The flat reference cell (F75) was built on flat glass and the textured reference cell (T75) was deposited on a commercial standard Asahi U-type glass. The short-circuit current density ( $J_{sc}$ ) of the nanorod cells is 1.7 and 1.4 times higher than that of the planar and the textured reference cells, respectively. An open-circuit voltage ( $V_{oc}$ ) of 0.79 V is observed in the nanorod devices with a fill factor of 0.55, both of which are slightly smaller than these parameters in the two reference cells. Figure 2(b) exhibits the corresponding external collection efficiency (ECE). As expected from the  $J_{sc}$  values in Fig. 2(a), a broad ECE profile with a maximum of 0.58 at around 470 nm is obtained for the nanorod devices. This is significantly higher than that obtained for the planar and the textured devices. The ECE results demonstrate that more pho-

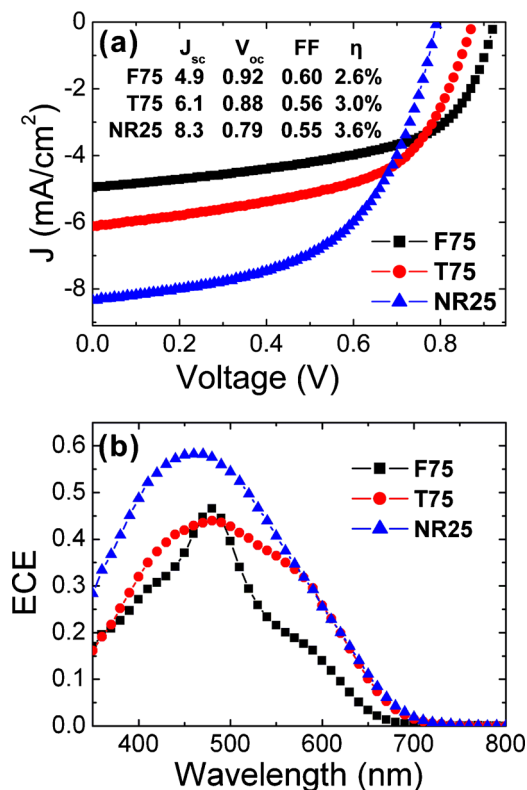


FIG. 2. (Color online) (a)  $J$ - $V$  measurements of the flat (F75), the textured (T75), and the nanorod (NR25) solar cells. Inset shows the cell characteristics for each device. (b) The corresponding spectral response curves.

togenerated charge-carriers are effectively collected in the nanorod devices, due to the thinner i-layer thickness and the unique nano-3D geometry.

In the nanorod solar cells, however, the unique nano-3D geometry not only allows the absorber in the axial direction to capture deeply penetrating photons (the red part of the spectrum), but there is also considerable enhancement in the blue response, as can be seen in Fig. 2(b). The principle of orthogonalization of light absorption and carrier collection in our nanorod system is similar to that in Kelzenberg *et al.*'s Si nanowire arrays<sup>19</sup> and Zhu *et al.*'s Si nanocone arrays,<sup>4</sup> except that the present substrate is an inexpensive alternative that requires no lithographic patterning and no catalysts for growth of the vertical nanorods.

Bulk recombination and surface recombination in a semiconductor limit the  $V_{oc}$ .<sup>32</sup> For the planar and the textured structure, bulk recombination is dominating, whereas for the nanorod geometry, surface recombination adversely affects the  $V_{oc}$  due to the increased internal surface area in comparison to that in devices either on planar or textured surfaces.<sup>2,3,9,11</sup> This demonstrates that limitation of surface and interface states is crucial for further optimization of these nanorod cells.

In summary, we have demonstrated a nano-3D solar cell concept that was prepared without lithographic patterning. An energy conversion efficiency of 3.6% has been obtained for nanorod solar cells with an ultrathin (about 25 nm) a-Si:H absorber layer. The effective carrier generation in the nano-3D geometry results in a higher efficiency in the nanorod devices even though the absorber layer is three times thinner than that in the planar and the textured solar cells studied. The simple and scalable fabrication process makes our nanorod/a-Si:H design a scalable system for low-cost efficient photovoltaic applications in the future.

Y.K. acknowledges the financial support from China Scholarship Council (CSC) under Contract No. 2009615001.

<sup>1</sup>M. J. Naughton, K. Kempa, Z. F. Ren, Y. Gao, J. Rybczynski, N. Argenti, W. Gao, Y. Wang, Y. Peng, J. R. Naughton, G. McMahon, T. Paudel, Y. C. Lan, M. J. Burns, A. Shepard, M. Clary, C. Ballif, F. J. Haug, T. Söderström, O. Cubero, and C. Eminian, *Phys. Status Solidi (RRL)* **4**, 181 (2010).

<sup>2</sup>B. M. Kayes, H. A. Atwater, and N. S. Lewis, *J. Appl. Phys.* **97**, 114302 (2005).

<sup>3</sup>J. M. Spurgeon, H. A. Atwater, and N. S. Lewis, *J. Phys. Chem. C* **112**, 6186 (2008).

<sup>4</sup>J. Zhu, Z. Yu, G. F. Burkhard, C. M. Hsu, S. T. Connor, Y. Xu, Q. Wang, M. McGehee, S. Fan, and Y. Cui, *Nano Lett.* **9**, 279 (2009).

<sup>5</sup>Y. Lu and A. Lal, *Nano Lett.* **10**, 4651 (2010).

<sup>6</sup>J. Zhu, C. M. Hsu, Z. Yu, S. Fan, and Y. Cui, *Nano Lett.* **10**, 1979 (2010).

<sup>7</sup>Z. Fan, H. Razavi, J. Do, A. Moriwaki, O. Ergen, Y. L. Chueh, P. W. Leu, J. C. Ho, T. Takahashi, L. A. Reichertz, S. Neale, K. Yu, M. Wu, J. W. Ager, and A. Javey, *Nature Mater.* **8**, 648 (2009).

<sup>8</sup>J. Li, H. Y. Yu, S. M. Wong, G. Zhang, X. Sun, P. G. Q. Lo, and D. L. Kwong, *Appl. Phys. Lett.* **95**, 033102 (2009).

<sup>9</sup>D. Kieven, T. Dittrich, A. Belaidi, J. Tornow, K. Schwarzburg, N. Allsop, and M. Lux-Steiner, *Appl. Phys. Lett.* **92**, 153107 (2008).

<sup>10</sup>A. Belaidi, T. Dittrich, D. Kieven, J. Tornow, K. Schwarzburg, and M. Lux-Steiner, *Phys. Status Solidi (RRL)* **2**, 172 (2008).

<sup>11</sup>M. Krunk, E. Kärber, A. Katerski, K. Otto, I. O. Acik, T. Dedova, and A. Mere, *Sol. Energy Mater. Sol. Cells* **94**, 1191 (2010).

<sup>12</sup>M. Krunk, A. Katerski, T. Dedova, I. O. Acik, and A. Mere, *Sol. Energy Mater. Sol. Cells* **92**, 1016 (2008).

<sup>13</sup>M. Vanecek, N. Neykova, O. Babchenko, A. Purkrt, A. Poruba, Z. Remes, J. Holovsky, K. Hruska, J. Meier, and U. Kroll, European Photovoltaic Solar Energy Conference and Exhibition/5th World Conference on Photovoltaic Energy Conversion (2010), p. 2763.

- <sup>14</sup>V. Sivakov, G. Andrä, A. Gawlik, A. Berger, J. Plentz, F. Falk, and S. H. Christiansen, *Nano Lett.* **9**, 1549 (2009).
- <sup>15</sup>L. Tsakalakos, J. Balch, J. Fronheiser, B. A. Korevaar, O. Sulima, and J. Rand, *Appl. Phys. Lett.* **91**, 233117 (2007).
- <sup>16</sup>M. Law, L. E. Greene, J. C. Johnson, R. Saykally, and P. Yang, *Nature Mater.* **4**, 455 (2005).
- <sup>17</sup>Th. Stelzner, M. Pietsch, G. Andrä, F. Falk, E. Ose, and S. Christiansen, *Nanotechnology* **19**, 295203 (2008).
- <sup>18</sup>K. Peng, Y. Xu, Y. Wu, Y. Yan, S. T. Lee, and J. Zhu, *Small* **1**, 1062 (2005).
- <sup>19</sup>M. D. Kelzenberg, S. W. Boettcher, J. A. Petykiewicz, D. B. Turner-Evans, M. C. Putnam, E. L. Warren, J. M. Spurgeon, R. M. Briggs, N. S. Lewis, and H. A. Atwater, *Nature Mater.* **9**, 239 (2010).
- <sup>20</sup>B. Tian, X. Zheng, T. J. Kempa, Y. Fang, N. Yu, G. Yu, J. Huang, and C. M. Lieber, *Nature (London)* **449**, 885 (2007).
- <sup>21</sup>E. C. Garnett and P. Yang, *J. Am. Chem. Soc.* **130**, 9224 (2008).
- <sup>22</sup>B. D. Yuhas and P. Yang, *J. Am. Chem. Soc.* **131**, 3756 (2009).
- <sup>23</sup>E. Garnett and P. Yang, *Nano Lett.* **10**, 1082 (2010).
- <sup>24</sup>O. L. Muskens, J. G. Rivas, R. E. Algra, E. P. A. M. Bakkers, and A. Lagendijk, *Nano Lett.* **8**, 2638 (2008).
- <sup>25</sup>L. Vayssieres, *Adv. Mater. (Weinheim, Ger.)* **15**, 464 (2003).
- <sup>26</sup>L. E. Greene, M. Law, D. H. Tan, M. Montano, J. Goldberger, G. Somorjai, and P. Yang, *Nano Lett.* **5**, 1231 (2005).
- <sup>27</sup>L. E. Greene, B. D. Yuhas, M. Law, D. Zitoun, and P. Yang, *Inorg. Chem.* **45**, 7535 (2006).
- <sup>28</sup>L. E. Greene, M. Law, J. Goldberger, F. Kim, J. C. Johnson, Y. Zhang, R. J. Saykally, and P. Yang, *Angew. Chem., Int. Ed.* **42**, 3031 (2003).
- <sup>29</sup>C. Bekeny, T. Voss, H. Gafsi, J. Gutowski, B. Postels, M. Kreye, and A. Waag, *J. Appl. Phys.* **100**, 104317 (2006).
- <sup>30</sup>R. E. I. Schropp, K. F. Feenstra, E. C. Molenbroek, H. Meiling, and J. K. Rath, *Philos. Mag. B* **76**, 309 (1997).
- <sup>31</sup>M. K. van Veen, C. H. M. van der Werf, J. K. Rath, and R. E. I. Schropp, *Thin Solid Films* **430**, 216 (2003).
- <sup>32</sup>M. A. Green, *Solar Cells: Operating Principles, Technology, and System Applications* (Prentice-Hall, New Jersey, 1982).